Upper and lower plane bed definitions revised

Koji Ohata[1*] , Hajime Naruse[1] and Norihiro Izumi[2]

Abstract

Sedimentary structures in ancient deposits are clues to reconstruct past geohazards. While parallel lamination formed by plane beds is one of the most common sedimentary structures in event deposits such as turbidites, the formative conditions for plane beds remain unclear. In the literature, two types of plane beds (upper and lower plane beds) exist and are supposed to develop under different shear stresses, particle sizes, and flow regimes. Here, we present new phase diagrams based on the compilation of existing data regarding formative hydraulic conditions for plane beds to clarify the formation processes associated with the two types of plane beds. The diagrams indicated that the data form two separate populations and the gap between them corresponds to the threshold condition of the particle entrainment into suspension. Lower plane beds form when sediment particles move only as bed load. This phase space can be discerned from fine sand to gravel and differs from the conventional view in which the formation of the lower plane bed is limited to grain sizes above 0.7 mm. In addition, our phase diagrams suggest that upper plane beds appear under conditions of the active suspended load. Our analyses demonstrate that the suspended load contributes to the formation of plane beds, whereas other mechanisms can also produce fine-grained plane beds in flows with low bed shear stress. Thus, the results of this study suggest that the existing interpretations on fine-grained parallel lamination such as Bouma's T_d division need to be reconsidered. The bedform phase diagrams newly established in this study will be useful for estimating the flow conditions from the geologic records of event beds.

Keywords: Plane bed, Suspended load, Bed load, Bedform

1 Introduction

1.1 General introduction of bedforms

Sand grains on Earth surfaces are carried from mountains to deep seas by flows, e.g., river, winds, tidal flows, and sediment-laden gravity currents. The transport of these sediments is not only one of the primary processes of the Earth's surface material circulation, including the carbon cycle (Schlünz and Schneider 2000; Galy et al. 2007), but also a cause of severe geohazards such as landslides or debris flows. Such past geohazards can be reconstructed from the characteristics of their deposits (e.g., Mitra et al. 2021), suggesting the disaster risk of each region.

Interaction between flows and solid particles during sediment transport results in various morphologies including bedforms that display wavy or flat topographies. Bedforms have been found ubiquitously on sediment beds; for instance, in open-channel flows (e.g., Collinson 1970; Ma et al. 2017; Galeazzi et al. 2018) and oscillatory flows (e.g., Miller and Komar 1980; Masselink et al. 2007; Wu and Parsons 2019).

In the past decades, numerous laboratory experiments (e.g., Gilbert 1914; Guy et al. 1966; Southard 1991; Dumas et al. 2005; Perillo et al. 2014; Bradley and Venditti 2019) and field observations (e.g., Colby and Hembree 1955; van den Berg 1987; Cisneros et al. 2020) were conducted to obtain empirical relationships between flows and bedforms. Bedform phase diagrams have been used to understand the formation of bedforms in response to flow behavior (e.g., Chabert and Chauvin 1963; Southard and

*Correspondence: ohata.koji.24z@gmail.com
[1] Division of Earth and Planetary Sciences, Graduate School of Science, Kyoto University, Kitashirakawaoiwake-cho, Sakyo-ku, Kyoto-shi, Kyoto 606-8502, Japan
Full list of author information is available at the end of the article

Boguchwal 1990). Recently, Ohata et al. (2017) proposed bedform phase diagrams in three-dimensional parametric space, and their diagrams successfully characterized paleo-flow conditions from sedimentary structures.

1.2 Review of plane beds

Plane beds are bedforms that develop in various environments such as alluvial riverbeds (e.g., Hauer et al. 2019) and beach faces (e.g., Vaucher et al. 2018; Vaucher and Dashtgard 2021). The plane bed phase is characterized by nearly flat topography or low-relief bed waves. Flume experiments have explained that the migration of low-relief bed waves over plane beds results in planar lamination with a few millimeters in thick (Paola et al. 1989, Bridge and Best 1997). Planar lamination in sandstone beds (Fig. 1) is ubiquitously found in fluvial (e.g., Umazano et al. 2012; Mazumder and Van Kranendonk 2013), estuaries (e.g., Hori et al. 2001), tidal flat (e.g., Chakraborty et al. 2003), shoreface (e.g., Kikuchi 2018), and submarine fan environments (e.g., Eggenhuisen et al. 2011; Jobe et al. 2012). For example, deposits from turbidity currents (i.e., turbidites) in submarine environments exhibit succession of sedimentary structures called Bouma sequence, in which parallel lamination is observable in T_b and T_d divisions (Bouma 1962).

Fig. 1 Photographs showing planar lamination in sandy deposits. **A** Snapshot of a laboratory experiment conducted at Kyoto University. Flow is from right to left. Two types of sands ($D_{50}=0.12$ mm and 0.53 mm) were used. **B** Field photograph showing a turbidite sandstone in the Aoshima Formation of the Miocene Miyazaki Group, Japan

Plane beds were initially referred to as "the smooth phase of bedforms" (Owens 1908; Gilbert 1914). Later, Simons et al. (1961) used the term "plane" to avoid confusion with the hydraulically smooth phase of flows. Owens (1908) and Strahan et al. (1908) observed that the bed state changes from ripples to the smooth phase of bedform (i.e., plane bed) and then to antidunes with increasing flow velocity. In addition, the plane bed phase also appears under the condition when the bed shear stress is lower than that forming ripples or dunes (e.g., Simons et al. 1961; Southard 1971). Thus, previous studies have recognized that there are two conditions of plane bed formation and they are separated by formation conditions of ripples or dunes.

However, the formative process and conditions for phase transition of plane beds remain unclear. It is known that the plane bed is formed under two different hydraulic conditions, but the reason why the formation conditions are divided into two regions is not well understood. In previous studies, the two types of plane beds have been classified depending on the (1) sediment motion (Simons et al. 1961; Simons and Richardson 1962), (2) criticality of Froude number (Venditti 2013; Dey 2014), and (3) size of bed material and flow intensity (Allen 1968; Southard 1971).

Simons et al. (1961) recognized two conditions of plane bed in their flume experiments using the medium sand—plane beds with and without sediment motion. On the basis of the flume experiments with the two types of medium sand ($D=0.28$ mm and 0.45 mm), Simons et al. (1961) and Simons and Richardson (1961, 1962) classified alluvial flows based on bedforms into three regimes—a lower flow regime (plane beds without sediment movement, ripples, dunes with ripples superposed, and dunes), a transition zone (washed-out dunes), and an upper flow regime (plane beds with sediment movement, standing waves, antidunes, and chutes-and-pools). Simons et al. (1961) and Simons and Richardson (1962) recognized this sequence of flow regimes with the increase in flow intensity. The definition of Simons et al. (1961) has been employed in the analyses of bedforms (van Rijn 1984b; Julien and Raslan 1998). For example, the bedform stability diagram proposed by Colombini and Stocchino (2008) has described plane bed phases as plane beds without sediment motion and upper plane bed. Bradley and Venditti (2019) cited the phase diagram by Colombini and Stocchino (2008) and described the phase of plane beds without sediment motion as lower plane beds.

Although Simons et al. (1961) noted that flows change from the lower to upper flow regimes at a Froude number (Fr) less than unity, Venditti (2013) and Dey (2014) stated that lower and upper flow regimes are consistent with Froude-subcritical (Fr < 1) and Froude-supercritical

Ohata *et al. Progress in Earth and Planetary Science* (2022) 9:23

Page 3 of 13
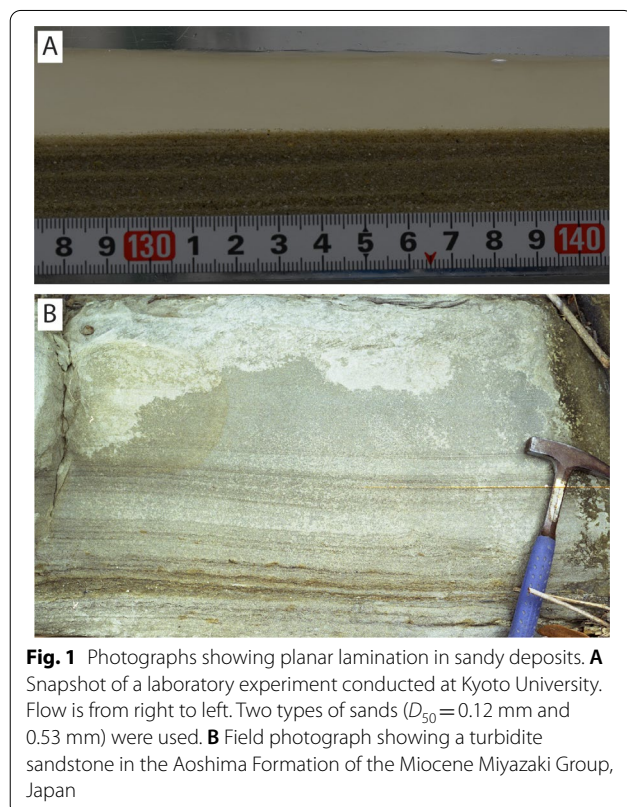
flow regimes (Fr > 1), respectively. In other words, following the definition by Venditti (2013) and Dey (2014), plane bed in the lower regime is generally interpreted to exist at Fr < 1, and plane bed in the upper regime is at or above Fr = 1.

Allen (1968) and Southard (1971) described bedform phase diagrams based on a compilation of observational data (Fig. 2). In their phase diagrams, there is a stable plane bed region where coarse sediment (median diameter D_{50} > 0.6–0.7 mm) is transported at low flow velocities (< 0.5 m/s). Allen (1968) termed this bed state as a lower-phase plane bed. That is, there are two types of plane beds with sediment movement, namely lower plane beds with low flow intensities on coarse sediment and upper plane beds with high flow intensities on fine sediment. Liu (1957) and Bogárdi (1961) also reported a region of flow conditions in which sediment motion occurred but ripples or other bedforms did not appear.

In summary, researchers have proposed various definitions and formation conditions of the two types of plane beds: (1) sediment motion (Simons et al. 1961; Simons and Richardson 1962), (2) criticality of Froude number (Venditti 2013; Dey 2014), and (3) size of bed material and flow intensity (Allen 1968; Southard 1971).

In this paper, we compiled a total of 935 sets of existing data from the literature. The dataset indicates that two separate regimes of plane bed exist and the boundary between the two plane bed regimes matches the threshold condition for the particle entrainment into suspension (Niño et al. 2003) or sheet flow (traction carpet; Gao 2008). We compiled data pertaining to plane beds in unidirectional open-channel flows and plotted them using dimensionless parameters as axes without any a priori

Fig. 2 Bedform phase diagram for unidirectional currents digitized after Southard and Boguchwal (1990) for a flow depth of 0.25–0.40 m. The mean velocity U_{10}, flow depth H_{10}, and grain size D_{10} denote 10 °C equivalent values

assumption of types of plane beds. Based on this data analysis, we recognized that the upper plane beds are always accompanied by suspension or sheet flow.

2 Methods

2.1 Data sources

We compiled from the literature a total of 935 sets of data pertaining to plane beds to investigate the plane bed regimes. The dataset consisted of 890 sets of laboratory data and 45 sets of field data (Tables 1 and 2). A wide range of hydraulic conditions and sediment calibers are encompassed in the datasets. The median sediment diameter (D_{50}) ranges from 1.1×10^{-2} to 44.3 mm, the flow depth (h) ranges from 1.2×10^{-3} to 2.74 m, and the flow velocity (U) ranges from 0.058 to 2.38 m/s. To compare the transport mode of plane bed formation with the threshold conditions of sediment motion and the initiation of suspension, we classified the data with sediment movement into three types based on the suspended sediment concentration (C_s), as follows: (a) The suspended sediment concentration was measured (hereafter referred to as data C_s > 0), (b) the suspended sediment concentration was recorded as zero (hereafter referred to as data C_s = 0), and (c) the suspended sediment concentration was not available (hereafter referred to as data no C_s).

2.2 Dimensionless parameters for morphodynamic conditions

First, we focused on the grain size and the sediment transport mechanism (i.e., no sediment movement, bed load, and suspended load) as controls on plane bed regimes. Bedform phases were expressed in a space of dimensionless parameters that reflected the properties of flows and sediment particles (e.g., van den Berg and van Gelder 1993; Ohata et al. 2017). We employed the following dimensionless parameters to represent hydraulic conditions and sediment properties: the particle Reynolds number (Re_p), Shields number (τ_*), and the suspension index (u_*/w_s).

The particle Reynolds number (Re_p) is defined as (Garcia 2000):

$$Re_p = \frac{\sqrt{RgD_{50}}D_{50}}{\nu} \qquad (1)$$

where R represents the submerged specific density of the sediment, g denotes the gravitational acceleration, and ν denotes the kinematic viscosity of the fluid. The submerged specific density is defined as $R = (\rho_s - \rho_f)/\rho_f$, where ρ_s and ρ_f represent the sediment and fluid densities, respectively. The kinematic viscosity (ν) was assumed to be a function of temperature according to the relationship for water (van den Berg and van Gelder 1993):
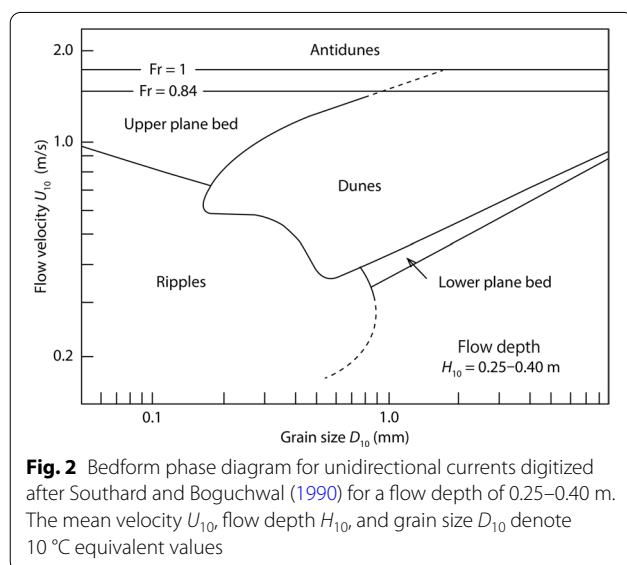
Table 1 Summary of flume data used for the analysis

Reference	# of points	Particle diameter D_{50} [mm]	Flow depth h [m]	Flow velocity U [m/s]	Particle Reynolds number Re_p	Shields number τ_*	Suspension index u_*/w_s	Froude number Fr
Barton and Lin (1955)*	11	0.18	0.13–0.24	0.74–1.09	9.74–11.1	0.47–1.13	1.7–2.88	0.52–0.87
Bridge and Best (1988)	2	0.3	0.1–0.1	0.9–0.98	19.85–21.86	1.29–1.38	1.98–2.02	0.91–0.99
Brooks (1955)*	8	0.09–0.15	0.06–0.09	0.6–0.65	3.7–8.63	0.43–0.77	1.98–5.03	0.71–0.81
Cao (1985)	84	11.5–44.3	0.02–0.26	0.31–1.64	4594–38,250	0.007–0.20	0.07–0.39	0.43–1.75
Chyn (1935)*	2	0.79	0.05–0.06	0.37–0.4	92.99–94.46	0.051–0.057	0.24–0.25	0.51
Costello (1974)*	8	0.6–0.79	0.15–0.16	0.32–0.39	72.28–103.48	0.019–0.055	0.14–0.26	0.26–0.31
E. Pakistan (1966, 68–69)*	4	0.25–0.33	0.15–0.3	0.19–0.86	17.66–28.31	0.019–0.46	0.21–1.27	0.11–0.71
Fukuoka et al. (1982)	18	0.19–1.6	0.02–0.07	0.35–1.19	10.52–256.97	0.037–0.76	0.18–1.3	0.61–2.12
Gee (1975)	3	0.31	0.08	0.94–1.02	21.73–23.12	0.47–0.55	1.16–1.21	1.06–1.17
Gilbert (1914)*	250	0.31–4.94	0.02–0.12	0.49–1.42	21.39–1393.27	0.062–0.90	0.22–1.42	0.79–2.08
Guy et al. (1966)	48	0.19–0.93	0.09–0.31	0.2–1.64	9.88–121.18	0.022–1.50	0.16–2.32	0.14–1.63
Jopling and Forbes (1979)	4	0.05	0.04–0.09	0.06–0.73	1.43–1.47	0.94–4.60	13.1–28.81	0.06–1.11
Jorissen (1938)*	9	0.6–0.91	0.02–0.09	0.26–0.44	57.79–118.26	0.045–0.097	0.22–0.34	0.43–0.59
Julien and Raslan (1998)	18	0.2–0.6	0.04–0.14	0.35–0.79	9.26–51.22	0.13–1.0	0.43–2.87	0.47–0.92
Kalinske and Hsia (1945)	1	0.01	0.16	0.83	0.15	8	347.79	0.67
Kennedy (1961)	12	0.23–0.55	0.02–0.11	0.61–1.05	15.68–60.75	0.36–0.62	0.81–1.57	0.73–2.04
Kennedy and Brooks (1963)	4	0.14	0.07–0.08	0.6–0.67	7.61–7.68	0.54–0.76	2.36–2.81	0.69–0.82
Kuhnle and Wren (2009)	2	0.5	0.17–0.18	0.68	44.89–45.3	0.41–0.64	0.81–1.02	0.51–0.53
Laursen (1958)	1	0.11	0.14	1.02	4.94	0.65	3.64	0.86
Mutter (1971)*	5	0.26	0.01–0.04	0.29–0.79	18.98–20.07	0.21–0.70	0.82–1.51	0.46–1.91
Neill (1967)**	30	5–20	0.03–0.18	0.5–1.13	1348.6–10,896.09	0.023–0.059	0.13–0.21	0.42–1.52
Nomicos (1956)*	12	0.09–0.15	0.07–0.08	0.56–0.81	3.89–8.93	0.42–0.83	1.96–4.52	0.66–0.95
Nordin (1976)	7	0.25–0.25	0.33–0.6	1.26–1.75	15.95–17.64	0.81–1.89	1.76–2.71	0.63–0.81
Pratt (1970)*	12	0.48	0.08–0.46	0.14–0.27	37.89–45.9	0.006–0.02	0.1–0.18	0.08–0.21
Rathbun and Guy (1967)	2	0.3	0.06–0.07	0.23–0.24	20.86	0.026–0.027	0.28–0.29	0.29
Singh (1960)*	30	0.62	0.01–0.07	0.28–0.8	51.98–60.15	0.042–0.56	0.24–0.88	0.4–1.2
Stein (1965)*	9	0.4	0.1–0.3	0.94–1.68	33.68–38.15	0.55–2.0	1–1.94	0.71–1.17
Taki and Parker (2005)	10	0.02–0.12	0.001–0.003	0.15–0.43	0.33–5.28	0.72–2.71	3.63–90.52	1.26–2.94
Tanaka (1970)	10	0.15–0.91	0.04–0.13	0.6–1.86	7.01–110.22	0.55–1.25	0.83–3.85	0.68–2.34
Taylor (1971)	31	0.14–3.95	0.06–0.18	0.2–0.88	7.61–1243.08	0.021–0.5	0.14–2.15	0.26–0.84
Ueno (1981)	8	0.23–0.6	0.01–0.03	0.21–0.31	12.48–56.86	0.031–0.08	0.21–0.65	0.52–0.6
U. S. W. Exp. Sta. (1935)*	75	0.18–4.1	0.01–0.12	0.25–0.68	8.97–1051.56	0.03–0.079	0.15–0.8	0.47–0.76
U. S. W. Exp. Sta. (1936)***	87	0.46–1.2	0.07–0.08	0.37–0.39	42.18–171.16	0.028–0.075	0.16–0.35	0.42–0.46
Vanoni and Brooks (1957)*	3	0.14	0.06–0.17	0.63–0.77	6.27–7.17	0.58–0.69	2.61–3.11	0.6–0.81
Williams (1970)	26	1.35	0.02–0.15	0.33–2.34	143.77–228.03	0.033–0.61	0.17–0.75	0.4–3.5
Willis et al. (1972)*	43	0.1	0.12–0.32	0.69–1.57	3.77–4.89	0.40–2.55	3.12–7.9	0.48–1
Znamenskaya (1963)*	1	0.18	0.09	0.71	9.7	0.47	1.87	0.77

Table 1 (continued)

*Cited from the dataset of Brownlie (2018). **Cited as Neill (1967) in Brownlie (2018). ***Cited as US Waterways Exp. Sta. (1936B) in Brownlie (2018)

Table 2 Summary of field data used for the analysis

References	# of points	particle diameter D_{50} [mm]	flow depth h [m]	flow velocity U [m/s]	Particle Reynolds number Re_p	Shields number τ_*	suspension index u_*/w_s	Froude number Fr
Baird (2010)	1	0.15	1.54	1.04	7.38	2.37	5.09	0.27
Colby and Hembree (1955)*	17	0.21–0.32	0.4–0.59	0.96–1.27	8.44–19.8	1.26–2.88	2.15–4.5	0.46–0.54
Culbertson et al. (1972)	14	0.16–0.24	0.28–1.11	0.46–1.66	5.38–17.82	0.48–2.08	1.3–5.14	0.26–0.52
Mahmood et al. (1979)*	6	0.08–0.21	1.46–2.32	0.6–0.8	3.57–9.71	0.60–1.45	2.1–7.01	0.13–0.19
Neill (1969)	3	0.34	0.91–2.74	0.67–1.01	20.81–20.81	0.45–1.34	1.16–2.01	0.19–0.22
Simons (1957)	4	0.03–0.36	1.32–1.83	0.59–0.64	0.66–30.93	0.25–2.77	0.74–46.94	0.14–0.17

*Cited from the dataset of Brownlie (2018)

$$\nu = \left[1.14 - 0.031(T - 15) + 0.00068(T - 15)^2 \right] 10^{-6} \tag{2}$$

where T represents the water temperature in degree Celsius. Following van den Berg and van Gelder (1993), we assumed a value of 20 °C for data where T was not reported. Shields number (τ_*) is defined as

$$\tau_* = \frac{u_*^2}{RgD_{50}} \tag{3}$$

Here, the shear velocity (u_*) for the field data was computed as $u_* = \sqrt{ghS}$, where S represents the bed slope. For laboratory data, we removed the sidewall effect and calculated the bed component of the shear velocity using the method proposed by Chiew and Parker (1994) (see Ohata et al. (2017) for details). We focused on the analysis of plane bed data in this study; therefore, we assumed the flow resistance induced by the bedforms is negligible.

The suspension index is expressed as the ratio of the shear velocity (u_*) to the settling velocity of sediment (w_s). The settling velocity was estimated using the relationship formulated by Ferguson and Church (2004):

$$w_s = \frac{RgD_{50}^2}{C_1\nu + \sqrt{0.75C_2RgD_{50}^3}} \tag{4}$$

where constants C_1 and C_2 were set to 18 and 1, respectively, which were the values for natural sands (Ferguson and Church 2004).

The sediment transport regimes are classified based on the transport mechanism—no sediment movement, bed-load-dominated, mixed-load, and suspended-load-dominated regimes (Church 2006). The boundary between

no sediment movement and other regimes is defined by the Shields curve, which is the critical condition for the initiation of particle motion (e.g., Shields 1936). Based on Shields' experimental data, Brownlie (1981) proposed a function describing the threshold condition of particle motion as:

$$\tau_{*c} = 0.22Re_p^{-0.6} + 0.06 \exp\left(-17.77Re_p^{-0.6} \right) \tag{5}$$

Next, the threshold condition for the initiation of suspension is expressed using the suspension index (u_*/w_s) (Bagnold 1966; van Rijn 1984a; Niño et al. 2003). The threshold condition of the particle entrainment into suspension represents the boundary between the bed-load-dominated regime and a regime where the bed materials are transported with suspension. The threshold condition for the particle entrainment into suspension, obtained by Niño et al. (2003), is:

$$\left(\frac{u_*}{w_s}\right)_c = \begin{cases} 21.2Re_p^{-1.2}, & 1 < Re_p < 27.3 \\ 0.4, & 27.3 \le Re_p \end{cases} \tag{6}$$

We used Eq. (5) (dashed line) and 6 (dotted line) to define the boundaries of the sediment transport regimes (Figs. 3, 4). The region on phase diagrams below the dashed line denotes the no sediment movement regime, the region between dashed and dotted lines denotes a bed-load-dominated regime, and the region above the dotted line denotes a mixed-load or suspended-load-dominated regime where bed materials are moved in bed load and suspension. To describe the threshold condition of sediment motion (Eq. 5) on the $Re_p - u_*/w_s$ diagram (Fig. 4) and the initiation of suspension (Eq. 6) on the $Re_p - \tau_*$ diagram (Fig. 3),

median sediment diameter D_{50} (mm)
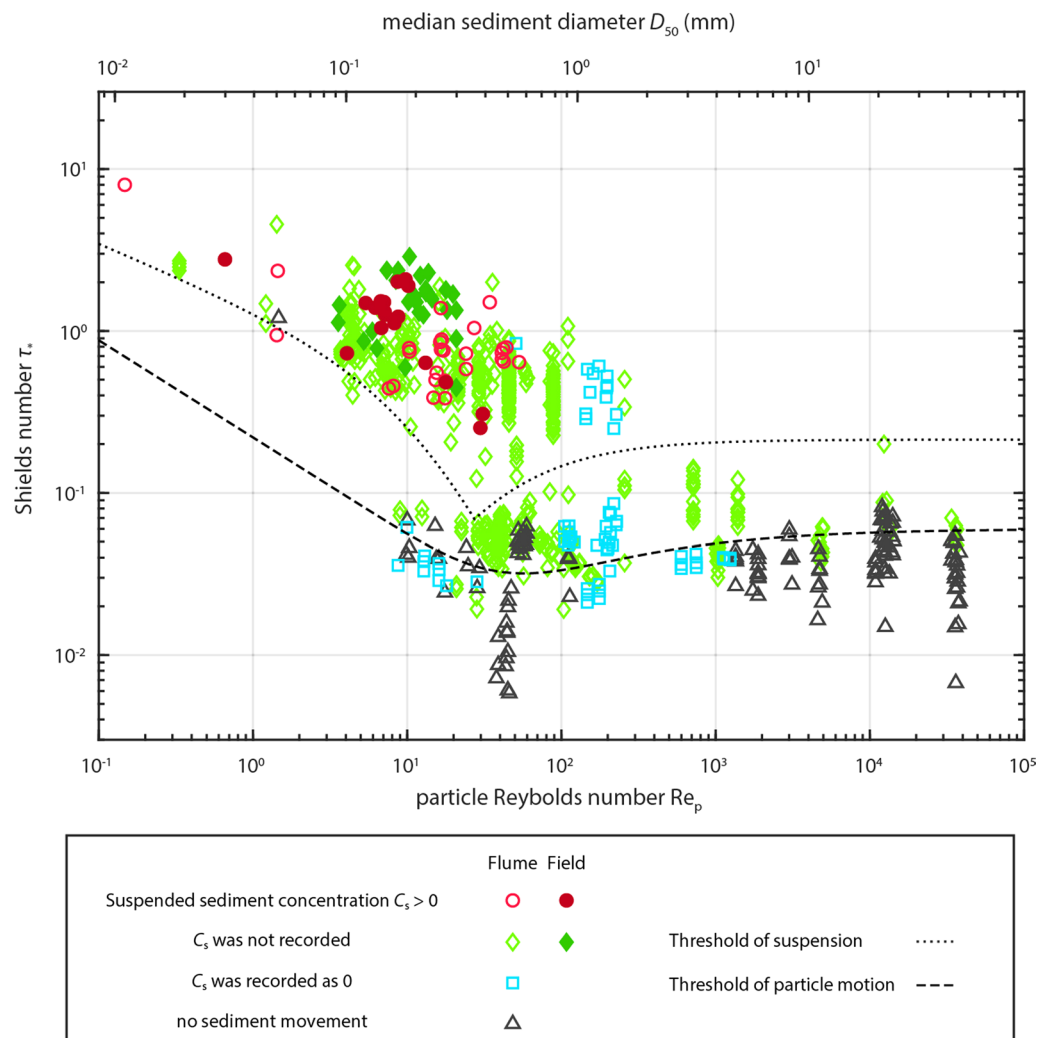
Fig. 3 Plane bed regime in a space of particle Reynolds number Re_p versus Shields number τ_*. The dotted line denotes the threshold condition for particle motion (Eq. 5). The solid line denotes the threshold condition for sediment suspension (Eq. 6). Both lines were extended to $Re_p = 10^{-1}$ and 10^5. The plane bed data are divided into two separate regions: the region around the threshold condition of particle motion and the region above the threshold condition of suspension

Eqs. (5 and 6) are rearranged using Eqs. (1, 3, and 4), where $R = 1.65$ (the value for quartz) and $\nu = 1.0 \times 10^{-6}$ (the value for water with 20 ℃).

Second, the plane bed conditions were investigated using Froude number. Phase diagrams were generated using Re_p, u_*/w_s, and Froude number as the axes. Froude number is the ratio of the inertial force to the gravitational force, defined as:

$$\mathrm{Fr} = \frac{U}{\sqrt{gh}} \tag{7}$$

3 Results
3.1 Influence of grain size and sediment transport mode

First, the plane bed data were plotted in $Re_p - \tau_*$ space (Fig. 3) to investigate the relationships among the plane bed regimes, the particle diameter, and the criteria for sediment movement. The threshold conditions of particle motion (Eq. 5) and suspension (Eq. 6) are shown in Fig. 3 as the dashed and dotted lines, respectively. The median diameter D_{50} is recast from Re_p with $R = 1.65$ and $\nu = 1.0 \times 10^{-6}$, which is represented on the top axis of Fig. 3.

Shields numbers associated with plane bed conditions range from 0.05 to 10, and the plane bed data are divided into two separate regions at $\tau_* = 0.1{-}0.2$
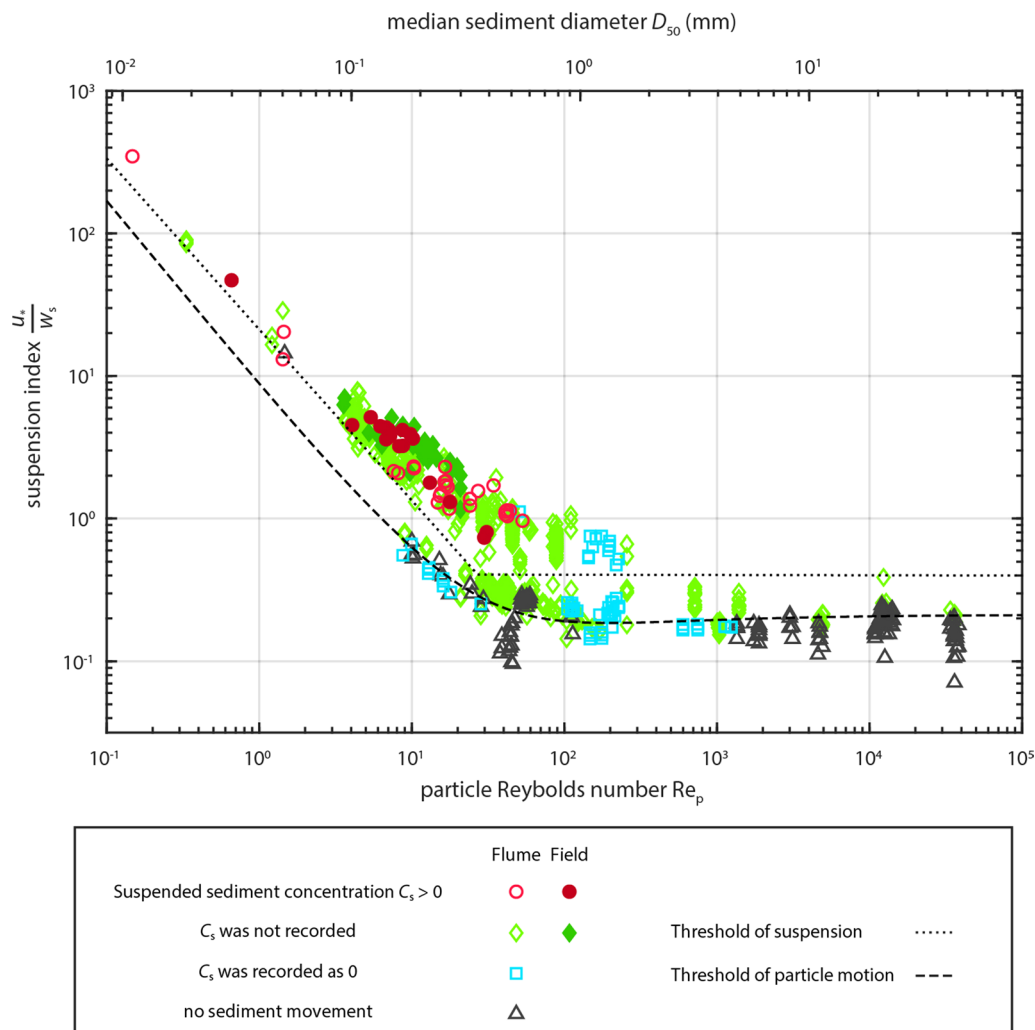
Fig. 4 Plane bed regime in a space of particle Reynolds number Re_p versus suspension index u_*/w_s. The dotted line denotes the threshold condition for particle motion (Eq. 5). The solid line denotes the threshold condition for sediment suspension (Eq. 6). Both lines were extended to $Re_p = 10^{-1}$ and 10^5. The plane bed data are divided into two separate regions: the region around the threshold condition of particle motion and the region above the threshold condition of suspension

(Fig. 3). The plane bed data with low τ_* plot around the threshold condition of particle motion, and the region with high τ_* plots above the threshold condition of suspension. The threshold condition of particle motion does not divide the plane bed regime; rather, the threshold condition of suspension runs between the two regions of data. The particle Reynolds numbers of the data with low τ_* range $9 < Re_p < 4.0 \times 10^4$ (0.2 mm $< D_{50} < 40$ mm). In the case of the data with high τ_*, the particle Reynolds number ranges from 0.1 to 300 (0.01 mm $< D_{50} < 2$ mm). The data $C_s > 0$ and field observation data are included in the region of high τ_*. The data $C_s = 0$ plot around the threshold condition for particle motion and $\tau_* = 0.4$.

Second, the relationships among the plane bed regimes, the sediment diameter, and the criteria for suspension were examined by plotting u_*/w_s versus Re_p (Fig. 4). Median diameter D_{50} is shown on the top axis of Fig. 4.

In Re_p-u_*/w_s space, the plane bed data plot in two regions separated by the threshold condition of suspension (Fig. 4), similar to our results in $Re_p-\tau_*$ space (Fig. 3). The threshold condition of particle motion runs through the middle of the data with a low suspension index. With respect to the particle Reynolds number, the data with a high suspension index plot in the region $0.1 < Re_p < 3.2 \times 10^3$ (0.01 mm $< D_{50} < 2$ mm) and the data with low suspension index plot in the region $9 < Re_p < 4.0 \times 10^4$ (0.2 mm $< D_{50} < 40$ mm).

The data $C_s > 0$ and field data plot above the threshold condition of suspension. The data $C_s = 0$ plot below and above the suspension criteria.

3.2 Effect of Froude number

We investigated the consistency of the flow regime concept based on Froude number (Venditti 2013; Dey 2014) to plane bed regimes, plotting data in Re_p–Fr space (Fig. 5). The data include Froude numbers ranging from 0.1 to 3.5. The data are not separated with regard to Froude number values. The field data have lower Froude numbers (Fr < 0.5) and higher Shields numbers and exceed the threshold condition of suspension (Figs. 3 and 4). For $C_s > 0$, the data fall in the domain 0.1 < Fr < 1.3 and the data $C_s = 0$ distribute in the domain 0.2 < Fr < 3.5.

4 Discussion

4.1 A new definition for plane beds

Data from the literature including field observations and flume experiments for plane beds were used to create phase diagrams for plane beds (Figs. 3, 4, 5). Traditionally, the particle diameters or the critical values of sediment motion or Froude number were used to discriminate lower and upper plane beds. However, our phase diagrams indicate that this is unlikely (Figs. 3, 4, 5). Indeed, the phase regions of the plane beds are not separated by the traditional indicators such as particle diameters. In contrast, observational data of the plane beds plot in two separate regions in the Re_p–τ_* and Re_p–u_*/w_s diagrams (Figs. 3, 4), and the boundary between the two regions corresponds to the threshold condition for sediment suspension. Therefore, we suggest that the upper and lower plane bed phases separated by the ripple and dune phases (Fig. 2) should be redefined—upper
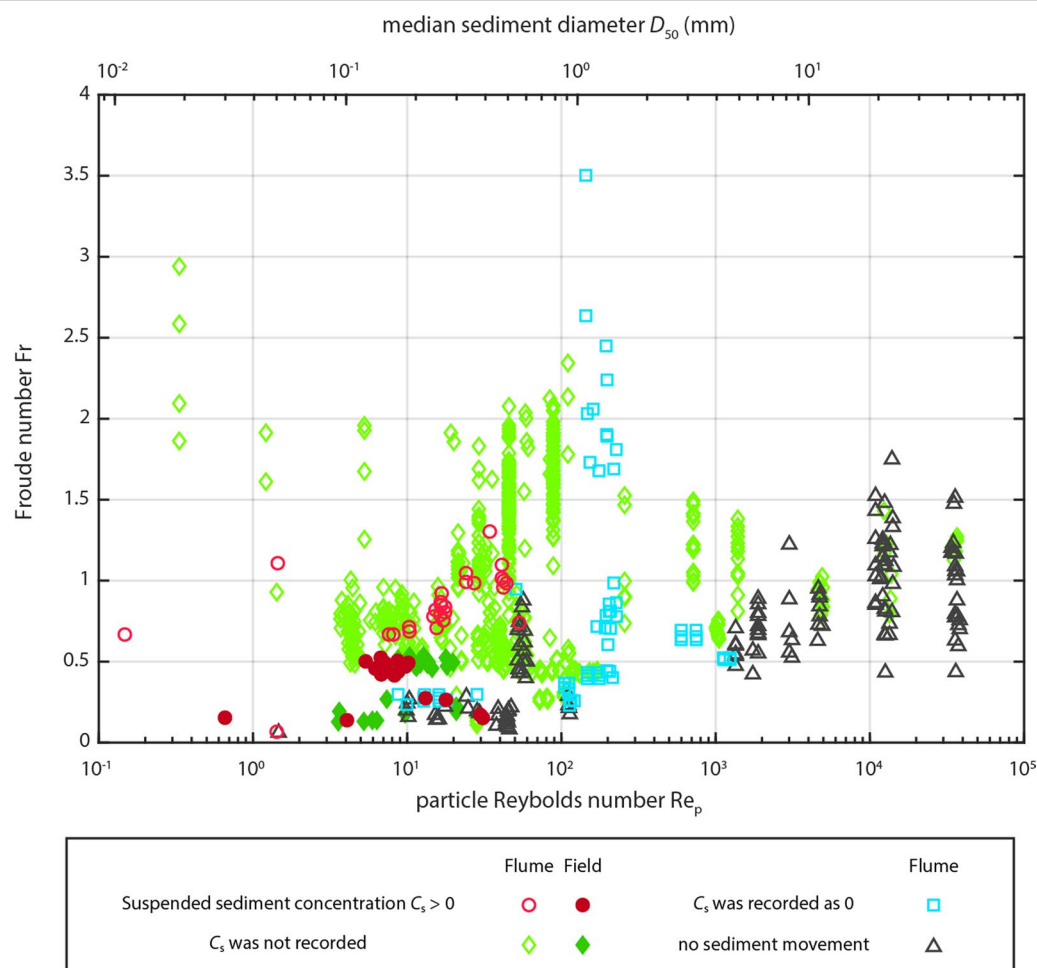
Fig. 5 Plane bed regime in a space of particle Reynolds number Re_p versus Froude number Fr. The data points of plane beds are not discriminated by Froude number

plane beds are plane beds in which the lower boundary is the threshold condition for sediment suspension, and lower plane beds are plane beds dominated by bed load. That is, there is a necessity to modify the classic bedform phase diagram.

Simons et al. (1961) defined lower plane beds as plane beds without sediment motion. For the data with a low Shields number ($\tau_* < 0.1$–0.2), there are overlaps of data points pertaining to plane beds with sediment movement and without sediment movement (Fig. 3). There is a range of shear stresses in which bed particles could move because, for example, the sediment bed is composed of natural sands that are somewhat angular and of various sizes. Hence, some data points of plane beds with sediment motion plotted below the line are defined by the threshold of sediment motion. Also, plane beds with sediment motion have been observed on a coarse-grained bed (Guy et al. 1966; Southard and Boguchwal 1973; Costello and Southard 1981; Cao 1985). These results of flume experiments demonstrate that the classical definition of plane beds by Simons et al. (1961) is not appropriate.

Similarly, Froude number cannot be used to discriminate the two types of plane beds (Fig. 5). Venditti (2013) and Dey (2014) stated that the upper and lower flow regimes are defined by Froude number. However, both plane beds with and without suspension can develop under various Froude numbers (Fig. 4). For example, plane beds appear with suspended loads in natural rivers where τ_* is high and Fr is less than unity due to the great depth (e.g., Ma et al. 2017). Therefore, we propose that lower and upper plane beds are not classified by the criticality of Froude number.

It is noteworthy that our analyses indicated that the regime of the lower plane bed extends to the region of fine-grained sediment (Figs. 3, 4). Southard (1971) defined lower plane beds as plane beds just above the threshold of sediment motion under subcritical flow with relatively coarse grains ($D_{50} > 0.7$ mm). Later, Southard and Boguchwal (1990) proposed bedform phase diagrams using a compilation of large datasets, although they omitted the data of relatively fine-grained plane beds (10 °C-equivalent sediment diameter is smaller than 0.7 mm) under low-velocity flows in their phase diagrams. Southard and Boguchwal (1990) did not include such data in their diagram because they suspected that equilibrium had not been attained. However, the duration of experiments performed by Guy et al. (1966) and Taylor (1971), which observed low-velocity plane beds in fine sediments, was from several hours to more than 24 h. The sediment discharge rates for low-velocity plane beds in the experiments of Guy et al. (1966) and Taylor (1971) are comparable to those of ripples in their experiments.

Further, the data points of low-flow velocity plane beds in fine sediment are continuous from those of low-flow velocity plane beds in coarse sediment (Figs. 3, 4). Therefore, the stable field of the plane bed without suspended load can be identified from fine sand to gravel.

The origin of the lower plane bed phase in the new definition is puzzling. In previous studies, one of the controlling factors in the lower and upper plane bed regimes was assumed to be the grain size and flow intensity (Allen 1968; Southard 1971). Leeder (1980) interpreted that coarse-grained plane beds are formed because flow separation is prevented by the bed roughness. Recently, Blois et al. (2014) proposed that bed permeability may be another explanation for the formation of coarse-grained plane beds. However, this study established that the region of coarse-grained plane beds extends continuously to the fine-grained region, and the conditions for fine-grained plane beds were distributed separately in the two regions: the high- and low-bed shear stresses. Thus, the formation of the lower plane bed cannot be attributed to bed roughness or permeability owing to the grain size distribution.

It should be noted here that bed particles are also transported in the sheet flow (traction carpet) regime (Sumer et al. 1996), which can be related to the plane bed. Sheet flows consist of a shear layer of bed load that moves under high shear stress ($\tau_* > \sim 0.5$) where ripples and dunes are washed out (Sumer et al 1996; Pugh and Wilson 1999). Williams (1970) observed that plane bed developed within sheet flows, and the data from Williams (1970) plotted above the threshold condition of suspension, yet no active suspension was observed in the experiments of Williams (1970) (Figs. 3, 4). Recently, Hernandez-Moreira et al. (2020) suggested that plane beds can develop under sheet flows in the intermediate condition between upstream and downstream migrating antidunes. However, experiments of sheet flow in open channels are scarce because laboratory experiments on sheet flows have been conducted using closed conduits in order to achieve high shear stresses (Nnadi and Wilson 1992; Sumer et al. 1996) or using oscillatory flow tunnels to simulate storm conditions (Dick and Sleath 1992; O'Donoghue and Wright 2004). Currently, it is difficult to determine whether sheet flow is another possible mechanism that generates plane beds. Further laboratory experiments, numerical experiments, and theoretical considerations are required to provide explanations for the plane bed regimes.

4.2 Theoretical explanation of plane bed formation

The transition from dunes to plane beds has been theoretically explained by the spatial lag between the dune crest and the location of maximum sediment transport

rate (Kennedy 1963). Dune height decreases when the maximum sediment transport rate occurs at the downstream of the dune crest. Recently, the spatial lag has been quantitatively observed under suspended-load-dominated flows (Naqshband et al. 2017), whereas there was no spatial lag in mixed-load flows (Naqshband et al. 2014). Therefore, the flume experiments by Naqshband et al. (2014, 2017) indicated that the increase in suspended load flux could lead to the spatial lag between the dune crest and the location of the maximum sediment transport rate. Figures 3 and 4 show the data of plane beds with suspension plotted at a region separated from the data of plane beds without suspension. That is, the compilation of the dataset supports that the spatial lag is caused by the existence of the suspended load.

Further, the influence of suspended load on the formation condition of bedforms has been demonstrated in the linear stability analyses by Nakasato and Izumi (2008). Nakasato and Izumi (2008) showed that the maximum Froude number for dune formation decreased by including the effect of suspended load; that is, the dune formation is partly suppressed. Although the results of linear analyses by Nakasato and Izumi (2008) were verified using the experimental data of dune and antidune of Guy et al. (1966), the hydraulic conditions of analyses were limited, and they did not make a comparison with the data of plane beds. In future theoretical research, it is required to analyze various conditions (e.g., sediment diameter and flow depth) and compare the results with the plane bed data.

4.3 Implication for rock record

Planar parallel lamination is often observed in ancient sedimentary successions and utilized to interpret the depositional environments (e.g., Clifton 1976; Plink-Björklund 2005). For example, planar-laminated sandstones from shallow marine conditions are interpreted to be formed in nearshore environments where wave collapse generates back-and-forth currents on the sea floor (Clifton 1976; Dumas and Arnott 2005; Vaucher et al. 2018).

In deep marine environments, turbidites may form planar laminations as the T_b and T_d divisions (Bouma 1962), although both may be absent (e.g., Sumner et al. 2012). The origin of the T_b division is attributed to plane bed deposition, whereas that of the T_d division is enigmatic (Middleton 1993; Talling et al. 2012). Following the definitions of Southard and Boguchwal (1990), Talling et al. (2012) argued that the origin of T_d division in turbidites is not the lower plane beds because the lower plane beds occur only on the coarse-grained beds. However, our phase diagrams imply that the origin of planar laminae in sandstone cannot be presumed

depending only on its particle size. Although Southard (1971) and Southard and Boguchwal (1990) suggested that lower plane beds cannot be formed with sediment finer than 0.7 mm in diameter, this study shows that fine-grained plane beds can develop at low-flow velocity (Figs. 3 and 4). Also, Hesse and Chough (1980) pointed out the possibility of the existence of fine-grained plane beds at low shear stress based on the flume experiments using silt-sized sediment by Rees (1966). Fine-grained plane beds can be stable at low shear stress because the critical shear stress to maintain the sediment movement under supersaturated flows where the sediment is already suspended is different from the critical shear stress to erode the sediment from the bed (Rees 1966). Also, T_d division is composed of silt- and clay-sized particles (Bouma 1962), and the cohesion is one of the possible mechanisms for the formation of plane beds in open-channel flows (Schindler 2015). Therefore, gaps in the existing data to explain the origin of T_d division should be filled by flume experiments of sediment-laden gravity currents and open-channel flows under controlled conditions.

5 Conclusions

In this study, we compiled 935 flume and field datasets pertaining to plane beds and analyzed the dataset in the nondimensional parametric space. The results of our analysis indicate that the formation conditions of plane beds do not show a clear boundary at the threshold condition of sediment motion, a unique value of particle diameter, or a Froude number of unity, which have been traditionally used to define lower and upper plane beds. Conversely, the formation conditions of plane beds are distributed in two separate regions, a lower plane bed dominated by bed load and an upper plane bed in which the lower boundary is the threshold condition for sediment suspension. This study demonstrates that suspended load significantly contributes to the formation of plane beds. Further experiments are needed to understand the mechanisms that can produce fine-grained plane beds in flows with low-bed shear stress.

Author contributions
KO proposed the topic and compiled the data. HN and NI contributed to the interpretation of the results. KO wrote the manuscript and prepared the figures, and then HN and NI provided feedback on the manuscript and figures. All authors read and approved the final manuscript.

Ohata *et al. Progress in Earth and Planetary Science*   (2022) 9:23

Page 11 of 13

Availability of data and materials
The data used for the analysis can be found at [url to be updated at acceptance]. Unpublished data used for the analysis were cited from the dataset of Brownlie (2018).

Declarations

Competing interests
The authors declare that they have no competing interests.

Author details
[1]Division of Earth and Planetary Sciences, Graduate School of Science, Kyoto University, Kitashirakawaoiwake-cho, Sakyo-ku, Kyoto-shi, Kyoto 606-8502, Japan. [2]Division of Field Engineering for the Environment, Faculty of Engineering, Hokkaido University, Kita-ku, Sapporo-shi, Hokkaido 060-8628, Japan.

References

Allen JRL (1968) Current ripples: their relation to patterns of water and sediment motion. North Holland Publishing Company, Amsterdam, p 433

Bagnold RA (1966) An approach to the sediment transport problem from general physics. U.S. Geological Survey Professional Paper 422-I

Baird DC (2010) Field adjustments of bed form phase diagrams. In: 2nd Joint federal interagency conference, Las Vegas, pp 1137–1145

Barton JR, Lin PN (1955) A study of the sediment transport in alluvial channels. Report CEF55JRB2. Colorado State University, Fort Collins

Blois G, Best JL, Sambrook Smith GH, Hardy RJ (2014) Effect of bed permeability and hyporheic flow on turbulent flow over bed forms. Geophys Res Lett 41:6435–6442. https://doi.org/10.1002/2014GL060906

Bogárdi J (1961) Some aspects of the application of the theory of sediment transportation to engineering problems. J Geophys Res 66:3337–3346. https://doi.org/10.1029/JZ066i010p03337

Bouma AH (1962) Sedimentology of some flysch deposits: a graphic approach to facies interpretation. Elsevier, Amsterdam, p 168

Bradley RW, Venditti JG (2019) Transport scaling of dune dimensions in shallow flows. J Geophys Res Earth Surf 124:526–547. https://doi.org/10.1029/2018JF004832

Bridge JS, Best JL (1988) Flow, sediment transport and bedform dynamics over the transition from dunes to upper-stage plane beds: implications for the formation of planar laminae. Sedimentology 35:753–763. https://doi.org/10.1111/j.1365-3091.1988.tb01249.x

Bridge J, Best J (1997) Preservation of planar laminae due to migration of low-relief bed waves over aggrading upper-stage plane beds: comparison of experimental data with theory. Sedimentology 44:253–262. https://doi.org/10.1111/j.1365-3091.1997.tb01523.x

Brooks NH (1955) Mechanics of streams with movable beds of fine sand. Proc Am Soc Civ Eng 81:1–28

Brownlie WR (1981) Prediction of flow depth and sediment discharge in open channels. Report KH-R43A, W.M. Keck Laboratory of Hydraulics and Water Resources, California Institute of Technology, Pasadena, California. https://doi.org/10.7907/Z9KP803R

Brownlie WR (2018) Digitized dataset from "Compilation of alluvial channel data: laboratory and field" (Version 1.0). CaltechDATA. https://doi.org/10.22002/d1.943

Cao HH (1985) Résistance hydraulique d'un lit à gravier mobile à penteraide: étude expérimentale. PhD thesis, Ecole Polytechnique Fédérale de Lausane, Switzerland

Chabert J, Chauvin JL (1963) Formation des dunes et des rides dans les modèles fluviaux. Bulletin du Centre de Recherches et d'Essais de Chatou

Chakraborty C, Ghosh SK, Chakraborty T (2003) Depositional record of tidal-flat sedimentation in the Permian coal measures of Central India: Barakar formation, Mohpani coalfield, Satpura Gondwana basin. Gondwana Res 6:817–827. https://doi.org/10.1016/S1342-937X(05)71027-3

Chiew YM, Parker G (1994) Incipient sediment motion on non-horizontal slopes. J Hydraul Res 32:649–660. https://doi.org/10.1080/00221689409498706

Church M (2006) Bed material transport and the morphology of alluvial river channels. Annu Rev Earth Planet Sci 34:325–354. https://doi.org/10.1146/annurev.earth.33.092203.122721

Chyn SD (1935) An experimental study of the sand transporting capacity of the flowing water on sandy bed and the effect of the composition of the sand. PhD thesis, Massachusetts Institute of Technology, Cambridge, Massachusetts

Cisneros J, Best J, van Dijk T, de Almeida RP, Amsler M, Boldt J, Freitas B, Galeazzi C, Huizinga R, Ianniruberto M, Ma H, Nittrouer JA, Oberg K, Orfeo O, Parsons D, Szupiany R, Wang P, Zhang Y (2020) Dunes in the world's big rivers are characterized by low-angle lee-side slopes and a complex shape. Nat Geosci 13:156–162. https://doi.org/10.1038/s41561-019-0511-7

Clifton HE (1976) Waveformed sedimentary structures—A conceptual model. In: Davis RA Jr, Ethington RL (eds) Beach and Nearshore Sedimentation. Society for Sedimentary Geology (SEPM) Special Publication 24, pp 126–148

Colby BR, Hembree CH (1955) Computations of total sediment discharge, Niobrara River Near Cody, Nebraska. U.S. Geological Survey Water-Supply Paper 1357

Collinson JD (1970) Bedforms of the Tana River, Norway. Geogr Ann Ser A Phys Geogr 52:31–56

Colombini M (2004) Revisiting the linear theory of sand dune formation. J Fluid Mech 502:1–16. https://doi.org/10.1017/S0022112003007201

Colombini M, Stocchino A (2008) Finite-amplitude river dunes. J Fluid Mech 611:283–306. https://doi.org/10.1017/S0022112008002814

Costello WR, Southard JB (1981) Flume experiments on lower-flow-regime bed forms in coarse sand. J Sediment Res 51:849–864. https://doi.org/10.1306/212F7DC4-2B24-11D7-8648000102C1865D

Costello WR (1974) Development of bed configuration in coarse sands. PhD thesis, Massachusetts Institute of Technology, Cambridge, Massachusetts

Culbertson JK, Scott CH, Bennett JP (1972) Summary of alluvial-channel data from Rio Grande conveyance channel, New Mexico, 1965–69. U.S. Geological Survey Professional Paper 562-J

Dey S (2014) Fluvial hydrodynamics: hydrodynamic and sediment transport phenomena. Springer, Germany, p 687

Dick JE, Sleath JFA (1992) Sediment transport in oscillatory sheet flow. J Geophys Res 97:5745–5758. https://doi.org/10.1029/92JC00054

Dumas S, Arnott RWC (2005) Origin of hummocky and swaley cross-stratification—the controlling influence of unidirectional current strength and aggradation rate. Geology 34:1073–1076. https://doi.org/10.1130/G22930A.1

Dumas S, Arnott RWC, Southard JB (2005) Experiments on oscillatory-flow and combined-flow bed forms: Implications for interpreting parts of the shallow-marine sedimentary record. J Sediment Res 75:501–513

East Pakistan Water and Power Development Authority (1966, 1968–1969) Flume studies of roughness and sediment transport of movable bed of sand. Annual Report of Hydraulic Research Laboratory, Dacca

Eggenhuisen JT, McCaffrey WD, Haughton PDW, Butler RWH (2011) Shallow erosion beneath turbidity currents and its impact on the architectural development of turbidite sheet systems. Sedimentology 58:936–959. https://doi.org/10.1111/j.1365-3091.2010.01190.x

Engelund F (1970) Instability of erodible beds. J Fluid Mech 42:225–244. https://doi.org/10.1017/S0022112070001210

Ferguson RI, Church M (2004) A simple universal equation for grain settling velocity. J Sediment Res 74:933–937. https://doi.org/10.1306/051204740933

Fukuoka S, Okutsu K, Yamasaka M (1982) Dynamic and kinematic features of sand waves in upper regime. In: Proceedings of the Japan Society of Civil Engineers, vol 323, pp 77–89 (**in Japanese**). https://doi.org/10.2208/jscej1969.1982.323_77

Galeazzi CP, Almeida RP, Mazoca CEM, Best JL, Freitas BT, Ianniruberto M, Cisneros J, Tamura LN (2018) The significance of superimposed dunes

Ohata *et al. Progress in Earth and Planetary Science* (2022) 9:23

Page 12 of 13

in the Amazon River: implications for how large rivers are identified in the rock record. Sedimentology 65:2388–2403. https://doi.org/10.1111/sed.12471

Galy V, France-Lanord C, Beyssac O, Faure P, Kudrass H, Palhol F (2007) Efficient organic carbon burial in the Bengal fan sustained by the Himalayan erosional system. Nature 450:407–410

Gao P (2008) Transition between two bed-load transport regimes: saltation and sheet flow. J Hydraul Eng 134:340–349. https://doi.org/10.1061/(ASCE)0733-9429(2008)134:3(340)

García MH (2000) Discussion of "The legend of A. F. Shields" by J. M. Buffington. J Hydraul Eng 126:718–720. https://doi.org/10.1061/(ASCE)0733-9429(2000)126:9(718)

Gee DM (1975) Bed form response to nonsteady flows. J Hydraul Div 101:437–449

Gilbert GK (1914) The transportation of debris by running water. U.S. Geological Survey Professional Paper 86

Guy HP, Simons DB, Richardson EV (1966) Summary of alluvial channel data from flume experiments, 1956–61. U.S. Geological Survey Professional Paper 462-I

Hauer C, Holzapfel P, Tonolla D, Habersack H, Zolezzi G (2019) In situ measurements of fine sediment infiltration (FSI) in gravel-bed rivers with a hydropeaking flow regime. Earth Surf Proc Land 44:433–448. https://doi.org/10.1002/esp.4505

Hernandez-Moreira R, Jafarinik S, Sanders S, Kendall CGSC, Parker G, Viparelli E (2020) Emplacement of massive deposits by sheet flow. Sedimentology 67:1951–1972. https://doi.org/10.1111/sed.12689

Hesse R, Chough SK (1980) The northwest atlantic mid-ocean channel of the Labrador Sea: II. Deposition of parallel laminated levee-muds from the viscous sublayer of low density turbidity currents. Sedimentology 27:697–711. https://doi.org/10.1111/j.1365-3091.1980.tb01656.x

Hori K, Saito Y, Zhao Q, Cheng X, Wang P, Sato Y, Li C (2001) Sedimentary facies of the tide-dominated paleo-Changjiang (Yangtze) estuary during the last transgression. Mar Geol 177:331–351. https://doi.org/10.1016/S0025-3227(01)00165-7

Jobe ZR, Lowe DR, Morris WR (2012) Climbing-ripple successions in turbidite systems: depositional environments, sedimentation rates and accumulation times. Sedimentology 59:867–898. https://doi.org/10.1111/j.1365-3091.2011.01283.x

Jopling AV, Forbes DL (1979) Flume study of silt transportation and deposition. Geografiska Annaler Ser A Phys Geogr 61:67–85. https://doi.org/10.2307/520516

Jorissen AL (1938) Étude expérimentale du transport solide des cours d'eau. Revue Universelle Des Mines 14:269–282

Julien PY, Raslan Y (1998) Upper-regime plane bed. J Hydraul Eng 124:1086–1096. https://doi.org/10.1061/(ASCE)0733-9429(1998)124:11(1086)

Kalinske AA, Hsia CH (1945) Study of transportation of fine sediments by flowing water. University of Iowa Studies in Engineering, Bulletin No. 29

Kennedy JF (1963) The mechanics of dunes and antidunes in erodible-bed channels. J Fluid Mech 16:521–544. https://doi.org/10.1017/S0022112063000975

Kennedy JF, Brooks NH (1963) Laboratory study of an alluvial stream of constant discharge. In: Proceedings of the Federal Inter-Agency Sedimentation Conference, pp 320–330

Kennedy JF (1961) Stationary waves and antidunes in alluvial channels. Report KH-R-2, W.M. Keck Laboratory of Hydraulics and Water Resources, California Institute of Technology, Pasadena, California. https://doi.org/10.7907/Z9QR4V22

Kikuchi K (2018) The occurrence of *Paleodictyon* in shallow-marine deposits of the Upper Cretaceous Mikasa Formation, Hokkaido Island, northern Japan: Implications for spatiotemporal variation of the *Nereites* ichnofacies. Palaeogeogr Palaeoclimatol Palaeoecol 503:81–89. https://doi.org/10.1016/j.palaeo.2018.04.016

Kuhnle RA, Wren DG (2009) Size of suspended sediment over dunes. J Geophys Res Earth Surf. https://doi.org/10.1029/2008JF001200.F02020

Laursen EM (1958) The total sediment load of streams. J Hydraul Div 84(1):1–36

Leeder MR (1980) On the stability of lower stage plane beds and the absence of current ripples in coarse sands. J Geol Soc 137(4):423–429. https://doi.org/10.1144/gsjgs.137.4.0423

Liu H-K (1957) Mechanics of sediment-ripple formation. J Hydraul Div 83:1–23

Ma H, Nittrouer JA, Naito K, Fu X, Zhang Y, Moodie AJ, Wang Y, Wu B, Parker G (2017) The exceptional sediment load of fine-grained dispersal systems: example of the Yellow River, China. Sci Adv. https://doi.org/10.1126/sciadv.1603114

Mahmood K, Tarar RN, Hassan SA, Khan H, Masood T (1979) Selected equilibrium-state data from ACOP canals. Report No. EWR-79-2. Civil, Mechanical and Environmental Engineering Department, George Washington University, Washington, DC

Masselink G, Austin MJ, O'Hare TJ, Russell PE (2007) Geometry and dynamics of wave ripples in the nearshore zone of a coarse sandy beach. J Geophys Res Oceans 112:C10022

Mazumder R, Kranendonk MJV (2013) Palaeoproterozoic terrestrial sedimentation in the Beasley River Quartzite, lower Wyloo Group, Western Australia. Precambr Res 231:98–105. https://doi.org/10.1016/j.precamres.2013.03.018

Middleton GV (1993) Sediment deposition from turbidity currents. Annu Rev Earth Planet Sci 21:89–114. https://doi.org/10.1146/annurev.ea.21.050193.000513

Miller MC, Komar PD (1980) A field investigation of the relationship between oscillation ripple spacing and the near-bottom water orbital motions. J Sed Res 50:183–191

Mitra R, Naruse H, Fujino S (2021) Reconstruction of flow conditions from 2004 Indian Ocean tsunami deposits at the Phra Thong island using a deep neural network inverse model. Nat Hazard 21:1667–1683

Mutter DG (1971) A flume study of alluvial bed configurations. Master's thesis, Faculty of Graduate Studies, University of Alberta, Edomonton, Alberta, Canada

Nakasato Y, Izumi N (2008) Linear stability analysis of small-scale fluvial bed waves with active suspended sediment load. J Appl Mech 11:727–734. https://doi.org/10.2208/journalam.11.727 (**in Japanese with English abstract**))

Naqshband S, Ribberink JS, Hurther D, Hulscher SJMH (2014) Bed load and suspended load contributions to migrating sand dunes in equilibrium. J Geophys Res Earth Surf 119:1043–1063. https://doi.org/10.1002/2013JF003043.2013JF003043

Naqshband S, Hoitink AJF, McElroy B, Hurther D, Hulscher SJMH (2017) A sharp view on river dune transition to upper stage plane bed. Geophys Res Lett 44:11437–11444. https://doi.org/10.1002/2017GL075906

Neill CR (1969) Bed forms in the lower Red Deer River, Alberta. J Hydrol 7:58–85. https://doi.org/10.1016/0022-1694(68)90195-9

Niño Y, Lopez F, Garcia M (2003) Threshold for particle entrainment into suspension. Sedimentology 50:247–263. https://doi.org/10.1046/j.1365-3091.2003.00551.x

Nnadi FN, Wilson KC (1992) Motion of contact-load particles at high shear stress. J Hydraul Eng 118:1670–1684. https://doi.org/10.1061/(ASCE)0733-9429(1992)118:12(1670)

Nomicos GN (1956) Effects of sediment load on the velocity field and friction factor of turbulent flow in an open channel. PhD thesis, California Institute of Technology, Pasadena, California

Nordin CF (1976) Flume studies with fine and coarse sands. U.S. Geological Survey, Open File Report No. 76-762

O'Donoghue T, Wright S (2004) Concentrations in oscillatory sheet flow for well sorted and graded sands. Coast Eng 50:117–138. https://doi.org/10.1016/j.coastaleng.2003.09.004

Ohata K, Naruse H, Yokokawa M, Viparelli E (2017) New bedform phase diagrams and discriminant functions for formative conditions of bedforms in open-channel flows. J Geophys Res Earth Surf 122:2139–2158. https://doi.org/10.1002/2017JF004290

Owens JS (1908) Experiments on the transporting power of sea currents. Geogr J 31:415–420

Paola C, Wiele S, Reinhart M (1989) Upper-regime parallel lamination as the result of turbulent sediment transport and low-amplitude bed forms. Sedimentology 36:47–59

Perillo MM, Best J, Garcia MH (2014) A new phase diagram for combined-flow bedforms. J Sediment Res 84:301–313

Plink-Björklund P (2005) Stacked fluvial and tide-dominated estuarine deposits in high-frequency (fourth-order) sequences of the Eocene Central Basin. Spitsbergen Sedimentol 52(2):391–428. https://doi.org/10.1111/j.1365-3091.2005.00703.x

Pratt CJ (1970) Summary of experimental data for flume tests over 0.49 mm sand. Department of Civil Engineering, University of Southampton, Southampton

Pugh FJ, Wilson KC (1999) Velocity and concentration distributions in sheet flow above plane beds. J Hydraul Eng 125:117–125. https://doi.org/10.1061/(ASCE)0733-9429(1999)125:2(117)

Rathbun RE, Guy HP (1967) Measurement of hydraulic and sediment transport variables in a small recirculating flume. Water Resour Res 3:107–122. https://doi.org/10.1029/WR003i001p00107

Rees AI (1966) Some flume experiments with a fine silt. Sedimentology 6:209–240. https://doi.org/10.1111/j.1365-3091.1966.tb01578.x

Schindler RJ, Parsons DR, Ye L, Hope JA, Baas JH, Peakall J, Manning AJ, Aspden RJ, Malarkey J, Simmons S, Paterson DM, Lichtman ID, Davies AG, Thorne PD, Bass SJ (2015) Sticky stuff: redefining bedform prediction in modern and ancient environments. Geology 43:399–402. https://doi.org/10.1130/G36262.1

Schlünz B, Schneider RR (2000) Transport of terrestrial organic carbon to the oceans by rivers: re-estimating flux-and burial rates. Int J Earth Sci 88:599–606

Shields A (1936) Application of similarity principles and turbulence research to bed-load movement (English translation of an original German manuscript). Soil Conservation Service Cooperative Laboratory, California Institute of Technology Pasadena, California (trans: Ott, WP and van Uchelen J. C.)

Simons, DB, Richardson, EV (1961) Forms of bed roughness in alluvial channels. J Hydraul Div 87

Simons DB, Richardson EV (1962) The effect of bed roughness on depth-discharge relations in alluvial channels. U.S. Geological Survey Professional Paper 1498-E

Simons DB, Richardson EV, Albertson ML (1961) Flume studies using medium sand (0.45 mm). U.S. Geological Survey Water-Supply Paper 1498-A

Simons DB (1957) Theory and design of stable channels in alluvial material. PhD thesis, Colorado State University, Fort Collins, Colorado

Singh B (1960) Transport of bed-load in channels with special reference to gradient and form. PhD thesis, University of London, London

Southard JB (1971) Representation of bed configurations in depth-velocity-size diagrams. J Sediment Res 41:903–915. https://doi.org/10.1306/74D723B0-2B21-11D7-8648000102C1865D

Southard JB (1991) Experimental determination of bed-form stability. Ann Rev Earth Planet Sci 19:423–455. https://doi.org/10.1306/74D72914-2B21-11D7-8648000102C1865D

Southard JB, Boguchwal LA (1973) Flume experiments on the transition from ripples to lower flat bed with increasing sand size. J Sediment Res 43:1114–1121. https://doi.org/10.1306/74D72914-2B21-11D7-8648000102C1865D

Southard JB, Boguchwal LA (1990) Bed configurations in steady unidirectional water flows. Part 2. Synthesis of flume data. J Sediment Petrol 60:658–679

Stein RA (1965) Laboratory studies of total load and apparent bed load. J Geophys Res 70:1831–1842. https://doi.org/10.1029/JZ070i008p01831

Strahan A, Lamplugh M, Cornish V, Mill D, Evans D, Tizard C, Creak C, Chisholm GG, Owens JS (1908) Experiments on the transporting power of sea currents: discussion. Geogr J 31:420–425

Sumer BM, Kozakiewicz A, Fredsøe J, Deigaard R (1996) Velocity and concentration profiles in sheet-flow layer of movable bed. J Hydraul Eng 122:549–558. https://doi.org/10.1061/(ASCE)0733-9429(1996)122:10(549)

Sumner EJ, Talling PJ, Amy LA, Wynn RB, Stevenson CJ, Frenz M (2012) Facies architecture of individual basin-plain turbidites: comparison with existing models and implications for flow processes. Sedimentology 59:1850–1887. https://doi.org/10.1111/j.1365-3091.2012.01329.x

Taki K, Parker G (2005) Transportational cyclic steps created by flow over an erodible bed. Part 1. Experiments. J Hydraul Res 43:488–501. https://doi.org/10.1080/00221680509500147

Talling PJ, Masson DG, Sumner EJ, Malgesini G (2012) Subaqueous sediment density flows: depositional processes and deposit types. Sedimentology 59:1937–2003. https://doi.org/10.1111/j.1365-3091.2012.01353.x

Tanaka Y (1970) An experimental study on anti-dunes. Disast Prevent Res Inst Ann 13B:271–284

Taylor BD (1971) Temperature effects in alluvial streams. Report KH-R-27, W.M. Keck Laboratory of Hydraulics and Water Resources, California Institute of Technology, Pasadena, CA. https://doi.org/10.7907/Z93776PN

United States Army Corps of Engineers, U.S. Waterways Experiment Station, Vicksburg, Mississippi (1935) Studies of river bed materials and their movement with special reference to the lower Mississippi River, p 161

Ueno T (1981) On the regions of occurrence of ripples and dunes. Proc Jpn Conf Hydraul 25:93–98. https://doi.org/10.2208/prohe1975.25.93 (**(in Japanese)**)

Umazano AM, Bellosi ES, Visconti G, Melchor RN (2012) Detecting allocyclic signals in volcaniclastic fluvial successions: facies, architecture and stacking pattern from the Cretaceous of central Patagonia, Argentina. J S Am Earth Sci 40:94–115. https://doi.org/10.1016/j.jsames.2012.09.005

van den Berg JH (1987) Bedform migration and bed-load transport in some rivers and tidal environments. Sedimentology 34:681–698. https://doi.org/10.1111/j.1365-3091.1987.tb00794.x

van den Berg JH, van Gelder A (1993) A new bedform stability diagram, with emphasis on the transition of ripples to plane bed in flows over fine sand and silt. In: Marzo M, Puigdefabregas C (eds) Alluvial sedimentation. Blackwell Scientific Publications, vol 17. International Association of Sedimentologists, pp 11–21

van Rijn LC (1984a) Sediment transport, part II: suspended load transport. J Hydraul Eng 110:1613–1641. https://doi.org/10.1061/(ASCE)0733-9429(1984)110:11(1613)

van Rijn LC (1984b) Sediment transport, part III: bed forms and alluvial roughness. J Hydraul Eng 110:1733–1754. https://doi.org/10.1061/(ASCE)0733-9429(1984)110:12(1733)

Vanoni VA, Brooks NH (1957) Laboratory studies of the roughness and suspended load of alluvial streams. Report E-68, W.M. Keck Laboratory of Hydraulics and Water Resources, California Institute of Technology, Pasadena, California

Vaucher R, Dashtgard SE (2021) Nearshore bedforms, reference module in earth systems and environmental sciences. Elsevier, Amsterdam

Vaucher R, Pittet B, Passot S, Grandjean P, Humbert T, Allemand P (2018) Bedforms in a tidally modulated ridge and runnel shoreface (Berck-Plage; North France): implications for the geological record. Bulletin De La Société Géologique De France. https://doi.org/10.1051/bsgf/2018004

Venditti JG (2013) Bedforms in sand-bedded rivers. In: Shroder J, Wohl E (eds) Treatise on geomorphology, vol 9. Academic Press, San Diego, pp 137–162

Williams GP (1970) Flume width and water depth effects in sediment transport experiments. U.S. Geological Survey Professional Paper 562-H

Willis JC, Coleman NL, Ellis WM (1972) Laboratory study of transport of fine sand. J Hydraul Div 98:489–501

Wu X, Parsons DR (2019) Field investigation of bedform morphodynamics under combined flow. Geomorphology 339:19–30

Znamenskaya NS (1963) Experimental study of the dune movement of sediment. In: Soviet hydrology: selected papers. American Geophysical Union, Washington, DC, pp 253–275

Publisher's Note